Analysis of Microstrip Circuits Using Three-Dimensional Full-Wave Electromagnetic Field Analysis in the Time Domain

TSUGUMICHI SHIBATA, MEMBER, IEEE, TOSHIO HAYASHI, AND TADAKATSU KIMURA, MEMBER, IEEE

Abstract—**Calculation of the frequency characteristics for microstrip circuits based on a three-dimensional full-wave electromagnetic field analysis in the time domain is proposed. In this method, the circuit is excited by a pulse which includes broadened frequency components. The frequency characteristics are then computed at once from the Fourier transform of the output transient responses. To evaluate the validity and capability of the method, a side-coupled microstrip filter is analyzed and the frequency characteristics are calculated. A quasi-static analysis of this filter is also presented and the results compared with measurements. The frequency characteristics calculated with the full-wave analysis in the time domain show excellent agreement with the measured values, thus demonstrating the validity and the power of the analytical method.**

I. INTRODUCTION

WITH THE DEVELOPMENT of high-speed device technology, it is becoming increasingly important to develop high-performance MMIC's which will serve as key components in compact and low-cost communication systems of the future. In MMIC's, microstrip circuits such as transmission lines (i.e., interconnect), filters, and couplers are used as circuit elements. Circuit designers are turning their attention to techniques for precisely analyzing their electrical properties. Some simple circuits have already been analyzed using quasi-static analysis. In most practical situations, however, because of the complicated electromagnetic fields that result from their three-dimensional shapes and locations, precise analysis cannot be expected from the more common analytical methods, or the so-called quasi-static analysis method. For greater accuracy, computer-aided numerical analysis of full-wave three-dimensional electromagnetic fields is required. This numerical analysis technique is thus an important key for the development of MMIC designs.

Two approaches have been taken with respect to full-wave electromagnetic field analysis. One is the time-domain analysis approach which solves the initial boundary value problem of the wave or Maxwell's equations. The other approach is a frequency-domain analysis method based on the eigenvalue problem of the vector Helmholtz equation. One of the advantages of the time-domain analysis, which is the main reason we have employed it here, is that the analysis is stable and yields a unique result, while the frequency-domain analysis suffers from spurious solutions and considerable care must be taken in the calculation process.

The numerical formulation of the time-domain analysis is given by Yee (the FD-TD method) [1], which uses finite difference equations of Maxwell's equations. An alternative method is based on the equivalent circuits of electromagnetic fields [2]. Johns *et al.* constructed an equivalent circuit with finite length transmission lines and developed a method of analysis based on the scattering matrix of each line (the T.L.M. method) [3]–[7]. These methods have been substantially modified in a number of reports [8]–[11]. Especially, Yoshida, Fukai and their coworkers have refined the T.L.M. method by expressing the medium constants by additional lumped elements to the equivalent circuit. They call their approach the Bergeron method. They also applied this method to the analysis of microstrip circuits and successfully showed the time variation of electromagnetic fields and power flow around the circuits [12]–[16]. But, for microstrip circuit design, it is necessary to calculate the frequency characteristics of the circuit. Since their analysis uses sinusoidal sources to excite the circuits, it is insufficient for this purpose.

The aim of this paper is to demonstrate calculation of the frequency characteristics for microstrip circuits and to establish the frequency-domain MMIC design method based on time-domain electromagnetic field analysis. The frequency characteristics are calculated using a raised cosine pulse source and applying the Fourier transform to the transient response of the circuit. In this way the frequency characteristics can be obtained at once over the full range of frequencies, whereas only one point of the frequency characteristic can be given using a sinusoidal source. By comparing the computed results and measured

Manuscript received October 20, 1987; revised January 19, 1988.
The authors are with NTT LSI Laboratories, 3-1 Morinosato Wakamiya, Atsugi-shi, Kanagawa, 243-01, Japan.
IEEE Log Number 8821075.

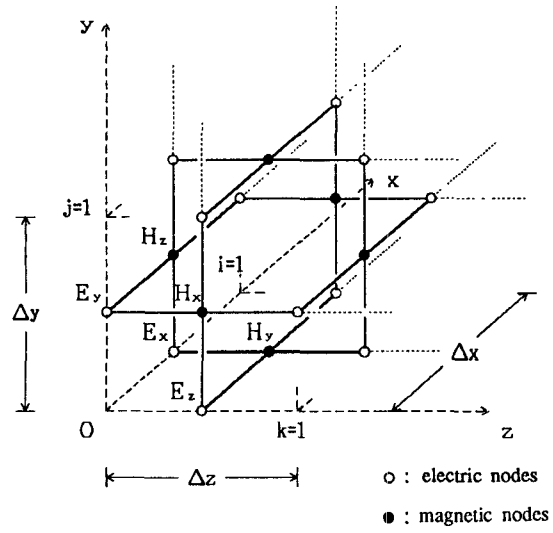

Fig. 1. The net of an equivalent circuit. Electric nodes,

$$E_x\left(i+\frac{1}{2},j,k\right),\quad i=0,1,\cdots,L-1;\ j=0,1,\cdots,M;\ k=0,1,\cdots,N$$

$$E_y\left(i,j+\frac{1}{2},k\right),\quad i=0,1,\cdots,L;\ j=0,1,\cdots,M-1;\ k=0,1,\cdots,N$$

$$E_z\left(i,j,k+\frac{1}{2}\right),\quad i=0,1,\cdots,L;\ j=0,1,\cdots,M;\ k=0,1,\cdots,N-1$$

and magnetic nodes,

$$H_x\left(i,j+\frac{1}{2},k+\frac{1}{2}\right),\quad i=0,1,\cdots,L;\ j=0,1,\cdots,M-1;\ k=0,1,\cdots,N-1$$

$$H_y\left(i+\frac{1}{2},j,k+\frac{1}{2}\right),\quad i=0,1,\cdots,L-1;\ j=0,1,\cdots,M;\ k=0,1,\cdots,N-1$$

$$H_z\left(i+\frac{1}{2},j+\frac{1}{2},k\right),\quad i=0,1,\cdots,L-1;\ j=0,1,\cdots,M-1;\ k=0,1,\cdots,N$$

are indicated by open circles and closed circles, respectively.

data, the time-domain analysis scheme can be verified. A side-coupled microstrip filter will be analyzed as an example to demonstrate the practicality of the scheme.

In the next section (Section II), we will briefly review the Bergeron method. The analysis of a single microstrip line is described in Section III as a preliminary to the analysis of a side-coupled microstrip filter in Section IV. In Section V, the results of the quasi-static analysis are presented and the necessity of the full-wave analysis is emphasized. In Section VI, we will discuss the accuracy of the full-wave, time-domain analysis. Finally, a few concluding remarks will be offered in Section VII.

II. The Equivalent Circuit of the Electromagnetic Field and Numerical Scheme of Analysis

In this section, we review the Bergeron method [12], which is used to solve for three-dimensional electromagnetic fields in the time domain using the equivalent circuits of the fields. Fig. 1 shows an equivalent circuit disposed in three-dimensional space. There are six kinds of nodes in the equivalent circuit: three electric nodes, E_x, E_y, and E_z, which are indicated by open circles in the figure, and three magnetic nodes H_x, H_y, and H_z, shown as closed circles. Branches consist of $\Delta l/2$ length transmission lines and gyrators, as shown in detail in Fig. 2. Values of the dielectric constant ϵ and permeability μ are expressed in terms of lumped capacitances connected to the corresponding electric and magnetic nodes, respectively. Electromagnetic field components E_x, E_y, E_z and H_x, H_y, H_z correspond to the node voltages of the equivalent circuit V_x, V_y, V_z and V_x^*, V_y^*, V_z^*, respectively, at each point (the * denoting the variables at the magnetic nodes). Electromagnetic field analysis results in the calculation of this equivalent circuit response. Fig. 3 shows the equivalent circuit at the E_x node. The following equations describe the node voltages and branch currents at the E_x node.

$$V_x(i,j,k,t)+Z_0I_{yi}(i,j,k,t)=I_{yo}^*\left(i,j-\frac{1}{2},k,t-\Delta t\right)+Z_0V_z^*\left(i,j-\frac{1}{2},k,t-\Delta t\right) \tag{1}$$

$$V_x(i,j,k,t)-Z_0I_{yo}(i,j,k,t)=I_{yi}^*\left(i,j+\frac{1}{2},k,t-\Delta t\right)-Z_0V_z^*\left(i,j+\frac{1}{2},k,t-\Delta t\right) \tag{2}$$

$$V_x(i,j,k,t)+Z_0I_{zi}(i,j,k,t)=I_{zo}^*\left(i,j,k-\frac{1}{2},t-\Delta t\right)+Z_0V_y^*\left(i,j,k-\frac{1}{2},t-\Delta t\right) \tag{3}$$

$$V_x(i,j,k,t)-Z_0I_{zo}(i,j,k,t)=I_{zi}^*\left(i,j,k-\frac{1}{2},t-\Delta t\right)-Z_0V_y^*\left(i,j,k-\frac{1}{2},t-\Delta t\right) \tag{4}$$

$$V_x(i,j,k,t)-\frac{\Delta t}{4C(i,j,k)}I_c(i,j,k,t)=V_x(i,j,k,t-\Delta t)+\frac{\Delta t}{4C(i,j,k)}I_c(i,j,k,t-\Delta t) \tag{5}$$

$$I_{yi}(i,j,k,t)-I_{yo}(i,j,k,t)+I_{zi}(i,j,k,t)-I_{zo}(i,j,k,t)-I_c(i,j,k,t)=0 \tag{6}$$

where Z_0 is the characteristic impedance of the transmission line and C is given by

$$C=(\epsilon_s-1)\epsilon_0\Delta \tag{7}$$

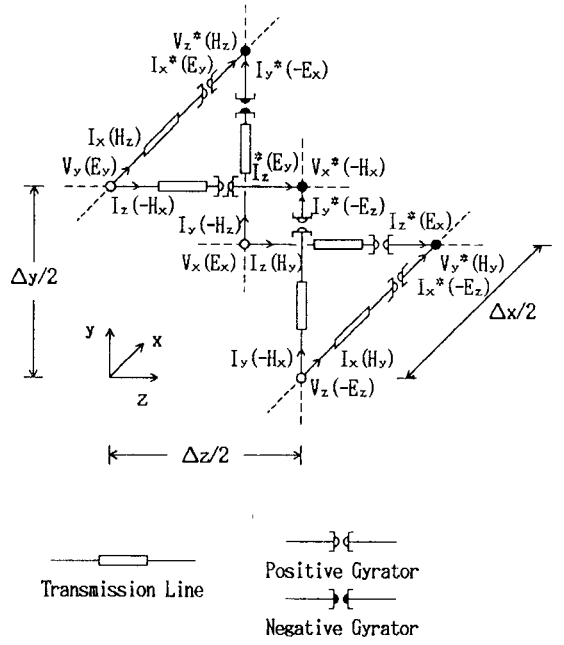

Fig. 2. Equivalent circuit elements. The equivalent circuit consists of finite length transmission lines and gyrators. $V-I$ characteristics of gyrators are

$$\begin{bmatrix} V \\ I \end{bmatrix} = \begin{bmatrix} 0 & 1 \\ 1 & 0 \end{bmatrix} \begin{bmatrix} V^* \\ I^* \end{bmatrix}$$

for the positive gyrator and

$$\begin{bmatrix} V \\ I \end{bmatrix} = \begin{bmatrix} 0 & -1 \\ -1 & 0 \end{bmatrix} \begin{bmatrix} V^* \\ I^* \end{bmatrix}$$

for the negative gyrator. Correspondence of circuit variables to electromagnetic field components is also shown in this figure.

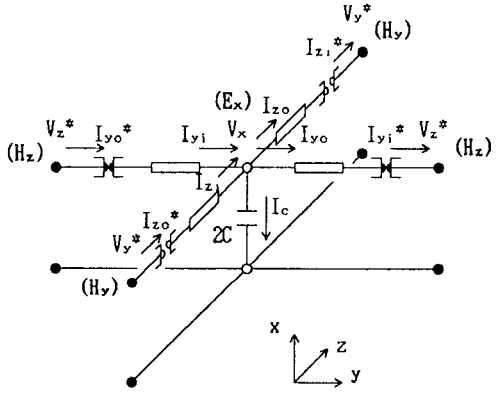

Fig. 3. Equivalent circuit at the E_x node.

at the electric nodes and

$$C = (\mu_s - 1)\mu_0 \Delta \tag{8}$$

at the magnetic nodes, where $\epsilon = \epsilon_s \epsilon_0$ and $\mu = \mu_s \mu_0$. The simulation time step Δt is related to the space distance Δ as

$$\Delta t = \frac{\Delta}{4c}. \tag{9}$$

We denoted the variables at the space point $x = i$, $y = j$, $z = k$ and at the time t as $V(i, j, k, t)$. Similar equations can be written relating to the E_y, E_z, H_x, H_y and H_z nodes. From these equations, we can calculate the node voltages at t from $t - \Delta t$.

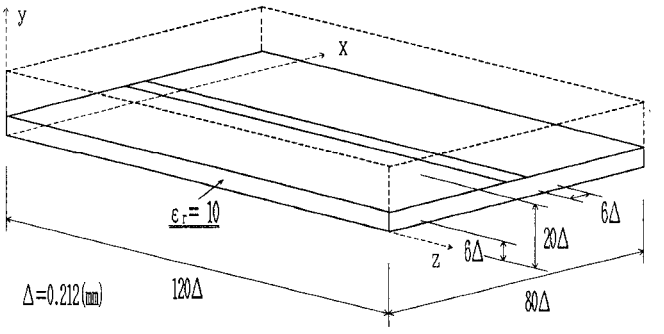

Fig. 4. Configuration of the single microstrip line.

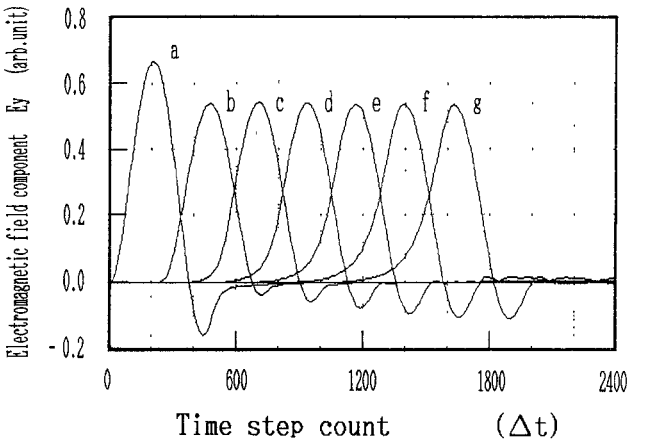

Fig. 5. The time variations of the electromagnetic field component E_y. The waves (a)–(g) are at the point $z = 0$, 20Δ, 40Δ, 60Δ, 80Δ, 100Δ, and 120Δ along the center line of the microstrip conductor in the substrate, respectively.

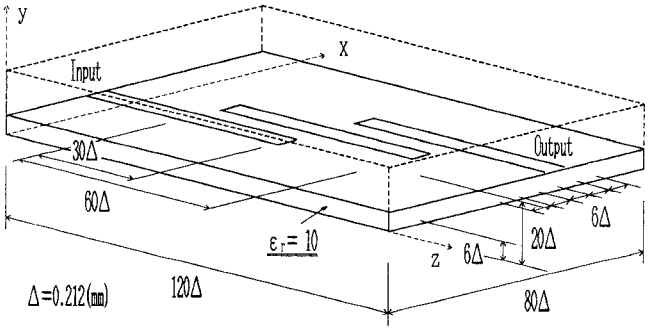

Fig. 6. Configuration of the side-coupled microstrip filter.

III. Analysis of a Single Microstrip Line

Prior to the description of a side-coupled microstrip filter, we discuss the results of a single microstrip line analysis. The configuration of the analyzed microstrip line is shown in Fig. 4. The net size of the equivalent circuit used here is $80\Delta x \times 20\Delta y \times 120\Delta z$ ($\Delta x = \Delta y = \Delta z = \Delta$). At the top and side faces of the equivalent circuit, irregular nodes are ended with matching impedances Z_0; thus, the infinite boundary condition is almost realized. The micro-

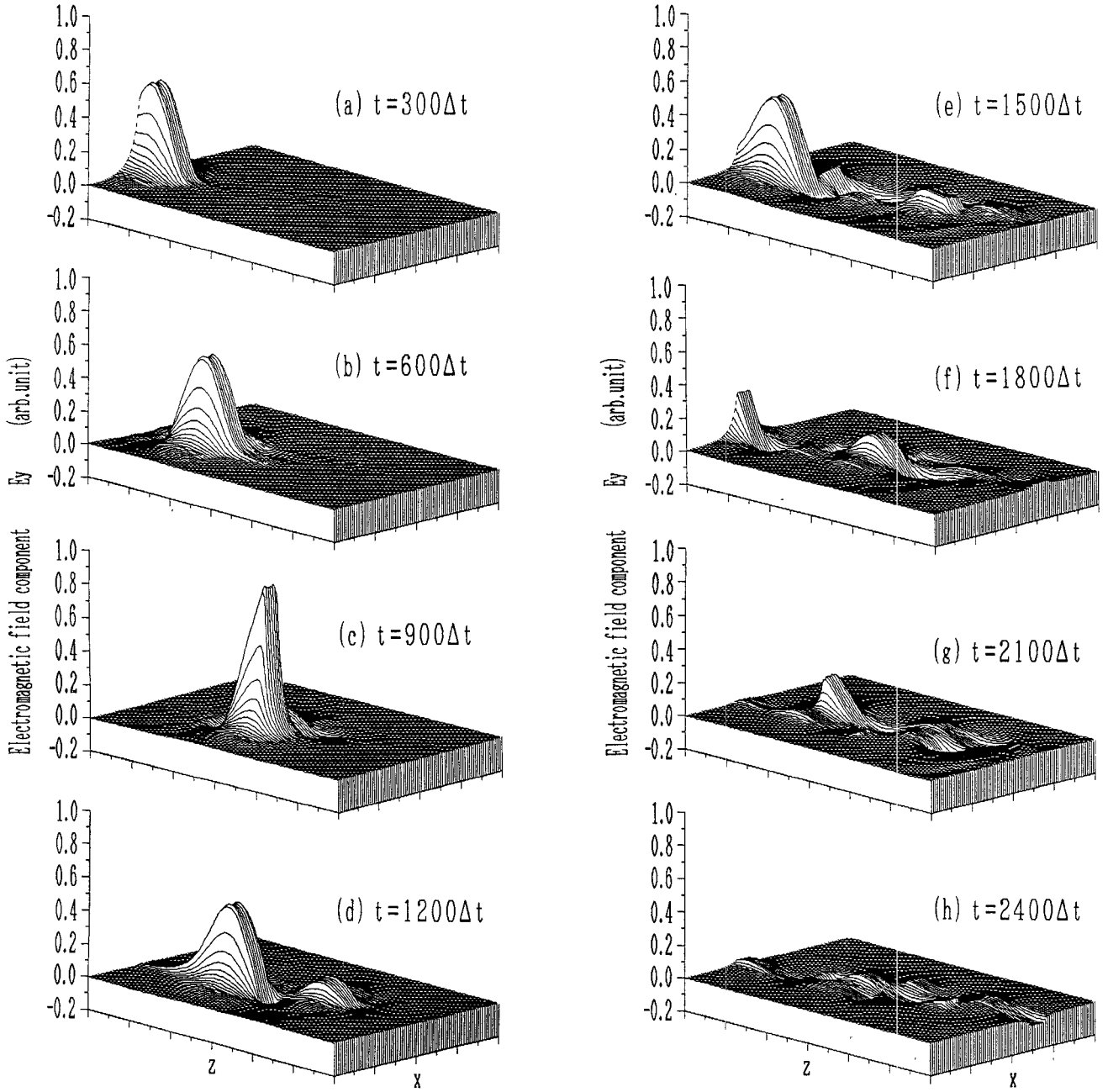

Fig. 7. The time variation of electromagnetic field component E_y at the $z-x$ plane in the substrate.

strip line parameters are as follows:

width of the microstrip conductor: $W = 6\Delta$;
thickness of the substrate: $H = 6\Delta$;
dielectric constant of the substrate: $\epsilon_r = 10.0$;
length of each transmission line in the equivalent circuit: $\Delta/2 = 0.106$ (mm).

Then, the simulation time step Δt becomes 0.176 (ps) from (9). The boundary conditions of the microstrip conductor and the bottom plane of the substrate are realized by short-circuiting the E_x and E_z nodes and open-circuiting the H_y node on the plane. As an input signal, a raised cosine pulse which equals a band-limited wave was adopted of the form

$$\begin{aligned} E_y(t) &= 1-\cos(2\pi f_{\text{band}} t) \quad \text{for } 0 \leqslant t < 1/f_{\text{band}} \\ &= 0 \quad \text{for } 1/f_{\text{band}} \leqslant t \\ f_{\text{band}} &= 11.8\ (\text{GHz}). \end{aligned} \tag{10}$$

Here, an internal impedance of Z_0 is applied to the E_y nodes under the microstrip conductor at the $z = 0$ plane, and initial values of the other field components are made zero. We applied only the E_y component under the microstrip line conductor to simplify the procedure instead of the total external electromagnetic field. The time variations of the electromagnetic field component E_y at the points under the center line of the microstrip conductor are plotted in Fig. 5.

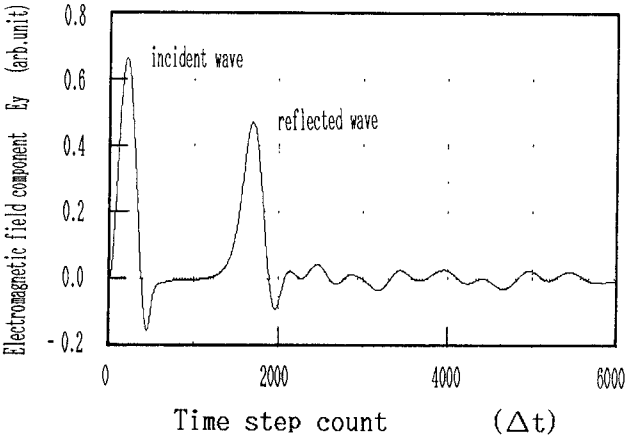

Fig. 8. The time variation of E_y at the input end.

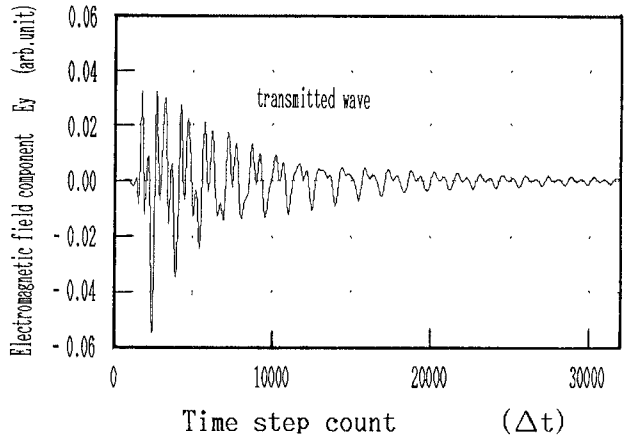

Fig. 9. The time variation of E_y at the output end.

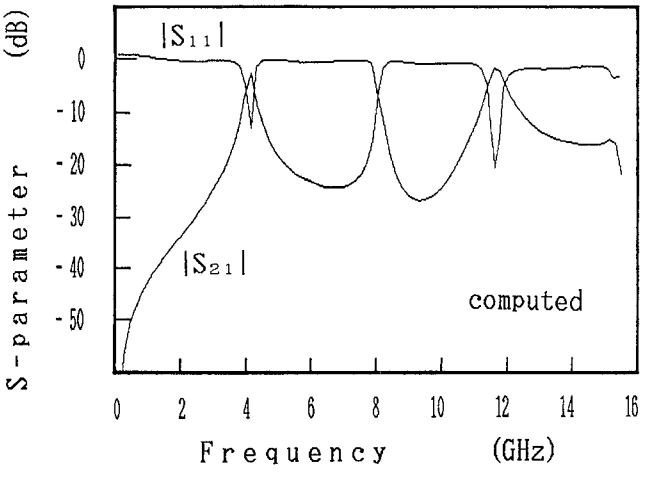

Fig. 10. Computed frequency characteristics of $|S_{21}|$ and $|S_{11}|$.

As a result of simplification of the input signal, the abrupt pulse height change from wave (a) to (b) has been reduced. The initial field component E_y was spread in space, thus creating a fringing field. The rest of the component was scattered and lost as radiation. The pulse height decreases rapidly near the input end and settles after propagating some distance (a few Δ lengths) along the microstrip in the z direction. At that point, the electromagnetic field distribution of the propagating mode is realized. We will take account of this pulse height reduction to calculate the frequency characteristics of the circuit in the next section.

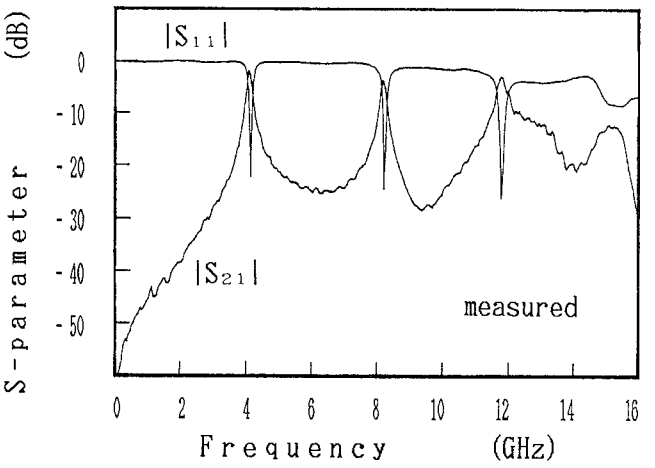

Fig. 11. Measured frequency characteristics of $|S_{21}|$ and $|S_{11}|$.

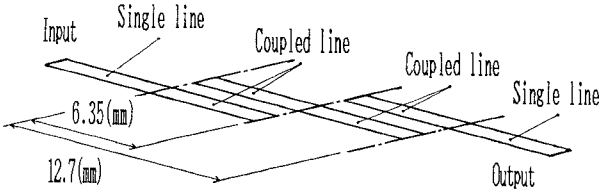

Fig. 12. Quasi-static analysis of the side-coupled microstrip filter. The filter is divided into four parts consisting of single and coupled lines.

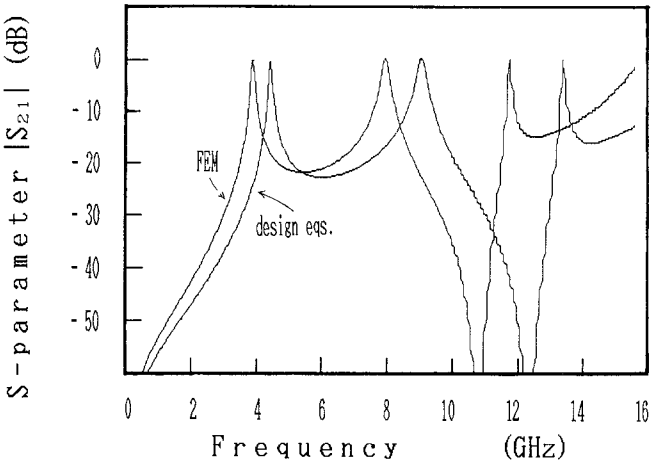

Fig. 13. The frequency characteristics of $|S_{21}|$ obtained by quasi-static analysis.

Notice also that the dispersion of the microstrip line can be simulated, which smoothes the slope of the pulse front and ripples the pulse tail because low-frequency components propagate faster than high-frequency components. Compare wave (g) with wave (b) in Fig. 5, for example.

IV. Analysis of a Side-Coupled Microstrip Filter

Here we describe the results of a side-coupled microstrip filter analysis. The configuration of the side-coupled microstrip filter is illustrated in Fig. 6. The width of the

TABLE I
PARAMETERS USED IN THE QUASI-STATIC ANALYSIS

	Single line		Coupled line			
	capacitance [pF/m]	inductance [nH/m]	self capacitance [pF/m]	mutual capacitance [pF/m]	self inductance [nH/m]	mutual inductance [nH/m]
Design equations	178.	422.	173.	11.0	420.	80.9
FEM	176.	469.	163.	11.8	572.	114.

microstrip line and the thickness and dielectric constant of the substrate are the same as the single microstrip line in the previous section. Other important size parameters are

space between microstrip conductors: $S = 6\Delta$;
length of the center microstrip conductor: $L = 60\Delta$.

The input signal given by (10) is applied at the input end and the electromagnetic field is computed step by step in time. The time variation of the electromagnetic field component E_y at the $z-x$ plane in the substrate is drawn in Fig. 7, in which (a)–(c) show that the incident wave propagates along the first microstrip conductor and is reflected at the end of the line. A part of the wave transfers to the center microstrip, while the reflected wave returns to the input end, in (d)–(e). The reflected wave fades away from view and the remainder resonates around the center microstrip in (f)–(g). The resonant component transfers to the third microstrip line and is transmitted to the output end in (h).

Figs. 8 and 9 are plots of E_y at input and output ends, respectively. From these waves, the frequency characteristics of the filter can be calculated. S parameters can be calculated from the Fourier transform of the reflected wave in Fig. 8 and the transmitted wave in Fig. 9, normalizing by the frequency spectrum of the incident wave (b) in Fig. 5 to correct the effect of the pulse height reduction discussed previously. Computed S parameters $|S_{11}|$ and $|S_{21}|$ are shown in Fig. 10.

In order to verify this computational method, we fabricated the side-coupled microstrip filter and measured $|S_{11}|$ and $|S_{21}|$ using the network analyzer. The results are shown in Fig. 11. The computed results show excellent agreement with the measured data.

V. The Results of Quasi-Static Analysis

In this section we describe the quasi-static analysis of the side-coupled microstrip filter which was previously analyzed using the time-domain, full-wave analysis. Then the findings based on the two different methods will be compared. Here the side-coupled microstrip filter is divided into four parts, consisting of single and coupled microstrip lines, as shown in Fig. 12. Single and coupled line parameters for a unit length can be estimated from static line capacitances on the assumption of TEM mode propagation. We calculated two sets of line capacitances from the design equations in [17] and the static field analysis using the finite element method (FEM) in [18]. The line inductance of the single line is calculated by

$$L = \frac{1}{c^2 C_{a\,r}}. \tag{11}$$

The self- and mutual inductances of the coupled line are given by

$$L_{self} = \frac{1}{2c^2}\left(\frac{1}{C_{self,air} - C_{mutual,air}} + \frac{1}{C_{self,air} + C_{mutual,air}}\right) \tag{12}$$

$$L_{mutual} = \frac{1}{2c^2}\left(\frac{1}{C_{self,air} - C_{mutual,air}} - \frac{1}{C_{self,air} + C_{mutual,air}}\right) \tag{13}$$

where c is the velocity of an electromagnetic wave in free space, and "air" means the capacitance of the line configuration with the dielectric substrate replaced by air. Calculated parameters are summarized in Table I. We obtained the $|S_{21}|$ of the side-coupled microstrip filter by circuit simulation using SPICE. The results are shown in Fig. 13. The differences between the inductances calculated by design equations and those by our numerical calculation using FEM range from 10 to 30 percent. However, both of the $|S_{21}|$ in Fig. 13 show the same tendency except for the scale of frequencies. Also important to note is that the results of quasi-static analysis are in disagreement with measured data, especially in the frequency domain over 8 GHz. These disagreements stem from the assumption of TEM mode propagation and/or from the separation of the filter into single and coupled lines. Thus, three-dimensional, full-wave analysis is needed for more precise computation.

VI. Discussion

We turn now to a consideration of the accuracy of frequency characteristic calculations using time-domain, full-wave analysis. Comparing the computed $|S_{11}|$ in Fig. 10 to the measured $|S_{11}|$ in Fig. 11, some difference in the peak level at the resonance point can be observed, resulting from the lack of frequency resolution. According to Fourier transform theory, frequency resolution Δf is given by the inverse of the observed time period T. On the other hand the time step Δt depends on the branch length $\Delta/2$, as shown in (9). Moreover, the length of Δ should be made small enough to express not only the shapes and locations of the microstrips but also the electromagnetic field distribution using the network variables. Our simulations using

other discretizations indicated that the accuracy of $|S_{21}|$, especially the resonance peak level around 8 GHz, depends on how many Δ's there are between microstrip lines. We need at least 5Δ lengths between isolated conductors. For this reason, it is important to make Δ sufficiently small, although it seems wasteful or oversampled to make the computational time step Δt too small and to require many iterations in time merely to obtain the frequency characteristics up to 16 GHz. To obtain the frequency characteristics shown in Fig. 10, we have computed the electromagnetic field distribution up to the $32768\Delta t$ time step. The resulting frequency resolution of Δf becomes 173 MHz.

VII. Conclusions

We propose an analysis method using pulse excitation in the time-domain, equivalent to a full-wave electromagnetic field analysis. The characteristics of a side-coupled microstrip filter were computed and excellent agreement with the measured values was obtained, thus confirming the validity of this analytical scheme. This example essentially requires the three-dimensional electromagnetic field treatment since no other method can provide the same level of precision. Moreover, the Bergeron method is effective for various media and is expected to produce various kinds of analysis, such as full-wave analysis in lossy conductors and dielectrics. Thus, the techniques described here are also promising for microstrip circuit analysis in the case of low conductivity of lines and/or semiconducting substrate.

Acknowledgment

The authors would like to thank Professor I. Fukai and Associate Professor N. Yoshida of Hokkaido University for their helpful discussions and A. Iwata, NTT LSI Laboratories, for his encouragement throughout this work.

References

[1] K. S. Yee, "Numerical solution of initial boundary value problems involving Maxwell's equations in isotropic media," *IEEE Trans. Antennas Propagat.*, vol. AP-14, pp. 302–307, May 1966.

[2] G. Kron, "Equivalent circuit of the field equations of Maxwell-I," *Proc. I.R.E.*, pp. 289–299, May 1944.

[3] P. B. Johns and R. L. Beurle, "Numerical solution of 2-dimensional scattering problems using a transmission-line matrix," *Proc. Inst. Elec. Eng.*, vol. 118, pp. 1203–1208, Sept. 1971.

[4] P. B. Johns, "The solution of inhomogeneous waveguide problems using a transmission-line matrix," *IEEE Trans. Microwave Theory Tech.*, vol. MTT-22, pp. 209–215, Mar. 1974.

[5] S. Akhtarzad and P. B. Johns, "Solution of Maxwell's equations in three space dimensions and time by t.l.m. method of numerical analysis," *Proc. Inst. Elec. Eng.*, vol. 122, pp. 1344–1348, Dec. 1975.

[6] S. Akhtarzad and P. B. Johns, "Generalised elements for t.l.m. method of numerical analysis," *Proc. Inst. Elec. Eng.*, vol. 122, pp. 1349–1352, Dec. 1975.

[7] P. B. Johns and G. Butler, "The consistency and accuracy of the TLM method for diffusion and its relationship to existing methods," *Int. J. Numer. Methods Eng.*, vol. 19, pp. 1549–1554, 1893.

[8] Y. Shih and W. J. R. Hoefer, "The accuracy of TLM analysis of finned rectangular waveguides," *IEEE Trans. Microwave Theory Tech.*, vol. MTT-28, pp. 743–746, July 1980.

[9] D. A. Al-Mukhtar and J. E. Sitch, "Transmission-line matrix method with irregularly graded space," *Proc. Inst. Elec. Eng.*, vol. 128, pp. 299–305, Dec. 1981.

[10] G. E. Mariki and C. Yeh, "Dynamic three-dimensional TLM analysis of microstrip- lines on anisotropic substrate," *IEEE Trans. Microwave Theory Tech.*, vol. MTT-33, pp. 789–799, Sept. 1985.

[11] W. J. R. Hoefer, "The transmission-line matrix method—Theory and applications," *IEEE Trans. Microwave Theory Tech.*, vol. MTT-33, pp. 882–893, Oct. 1985.

[12] N. Yoshida and I. Fukai, "Transient analysis of a stripline having a corner in three-dimensional space," *IEEE Trans. Microwave Theory Tech.*, vol. MTT-32, pp. 491–498, May 1984.

[13] S. Koike, N. Yoshida, and I. Fukai, "Transient analysis of microstrip gap in three-dimensional space," *IEEE Trans. Microwave Theory Tech.*, vol. MTT-33, pp. 726–730, Aug. 1985.

[14] S. Koike, N. Yoshida, and I. Fukai, "Transient analysis of a directional coupler using a coupled microstrip slot line in three-dimensional space," *IEEE Trans. Microwave Theory Tech.*, vol. MTT-34, pp. 353–357, Mar. 1986.

[15] S. Koike, N. Yoshida, and I. Fukai, "Transient analysis of microstrip side-coupled filter in three-dimensional space," *Trans. IECE Japan*, vol. E69, no. 11, pp. 1199–1205, Nov. 1986.

[16] S. Koike, N. Yoshida, and I. Fukai, "Transient analysis of coupling between crossing lines in three-dimensional space," *IEEE Trans. Microwave Theory Tech.*, vol. MTT-35, pp. 67–71, Jan. 1987.

[17] K. C. Gupta, R. Garg, and I. J. Bahl, *Microstrip Lines and Slotlines*. Dedham, MA: Artech House, 1979, pp. 87–89 and 337–340.

[18] P. Silvester, "High-order polynomial triangular finite elements for potential problems," *Int. J. Eng. Sci.*, vol. 7, pp. 849–861, 1969.

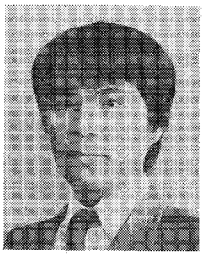

Tsugumichi Shibata (M'87) was born in Tokyo, Japan, on July 14, 1959. He received the B.S. and M.S. degrees in electrical engineering from Tokyo University, Tokyo, Japan, in 1983 and 1985, respectively.

In 1985, he joined the Atsugi Electrical Communications Laboratories, Nippon Telegraph and Telephone Corporation, Atsugi, Japan. He has been engaged in research on electromagnetic field analysis. His interests include the analysis of high-speed signals in MMIC's.

Mr. Shibata is a member of the Institute of Electronics, Information and Communication Engineers of Japan and the Japan Society of Applied Physics.

Toshio Hayashi was born in Toyama, Japan, on January 14, 1951. He received the B.S. and M.S. degrees in electronic engineering from the Nagoya Institute of Technology, Japan, in 1973 and 1975, respectively.

He joined NTT Electrical Communications Laboratories in 1975. He has been engaged in research and the design of high-speed bipolar memory LSI's and analog LSI's for communication use. He is now engaged in the research and development of analog CAD technology.

Mr. Hayashi is a member of the Institute of Electronics, Information and Communication Engineers of Japan.

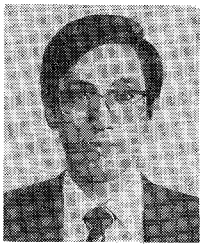

Tadakatsu Kimura (M'87) was born in Hokkaido, Japan, on August 20, 1945. He received the B.S. degree in engineering from the Muroran Institute of Technology, Muroran, Japan, in 1968.

He joined NTT Electrical Communications Laboratories in 1968. From 1968 to 1970 he did research on hybrid integration circuits, such as stripline circuits and microwave amplifiers. From 1971 to 1974 he was engaged in developmental research on high-speed hybrid integration circuits for PCM coaxial transmission-system repeaters. He is currently engaged in research on CMOS LSI for digital processing and analog LSI's for subscriber line interface circuits.

Mr. Kimura is a member of the Institute of Electronics, Information and Communication Engineers of Japan.